Multicolor and Electron Microscopic Imaging of Connexin Trafficking

Guido Gaietta,[1] Thomas J. Deerinck,[1] Stephen R. Adams,[2]
James Bouwer,[1] Oded Tour,[2]* Dale W. Laird,[3] Gina E. Sosinsky,[1]
Roger Y. Tsien,[2]* Mark H. Ellisman[1]†

Recombinant proteins containing tetracysteine tags can be successively labeled in living cells with different colors of biarsenical fluorophores so that older and younger protein molecules can be sharply distinguished by both fluorescence and electron microscopy. Here we used this approach to show that newly synthesized connexin43 was transported predominantly in 100- to 150-nanometer vesicles to the plasma membrane and incorporated at the periphery of existing gap junctions, whereas older connexins were removed from the center of the plaques into pleiomorphic vesicles of widely varying sizes. Selective imaging by correlated optical and electron microscopy of protein molecules of known ages will clarify fundamental processes of protein trafficking in situ.

To understand how genomes give rise to cells and organisms, one would like to be able to genetically tag any protein with a nonperturbing label visible both by nondestructive optical microscopy in live cells and by electron microscopy (EM) for higher spatial resolution. The jellyfish green fluorescent protein (GFP) and its mutants and homologs have provided solutions for optical imaging, but genetically encoded tags for electron microscopy are still lacking. Furthermore, if one could pulse-label a continuously expressed protein with one label and chase the staining with a different label, older and newer copies of the same species would be distinguishable in a single image, which would help to elucidate the mechanisms of assembly and turnover.
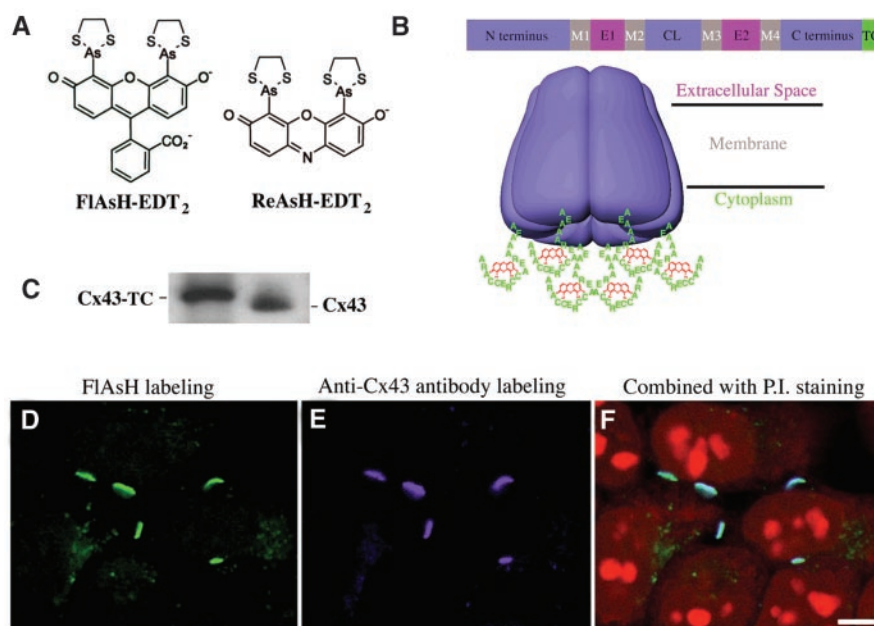
Important examples of dynamic structures created from a single family of proteins include gap junction plaques, which are composed of an array of tightly packed individual channels formed by the docking of two hemichannels (connexons) in the extracellular space between two contacting cells [reviewed in (1–3)]. Briefly, each cell provides one hemichannel, which is formed by six connexins arranged around a central pore. Plaques ensure direct communication between contacting cells by allowing small (less than 1 kD) signaling molecules, ions, and metabolites to pass directly from one cell to the other. This connectivity enables cells in tissues and organs to efficiently communicate in order to coordinate cellular activity. Because the degree of intercellular coupling is, for the most part, determined by the number of individual channels in a gap junction plaque, cells dynamically modulate this connectivity by regulating the synthesis, transport, and turnover of the constituent connexins, which have a half-life of less than 5 hours (4–7).

Much has been learned by tagging gap junctions through the fusion of fluorescent proteins like GFP to the COOH terminus of various connexins (8–11). However, GFP and its variants are 25 to 27 kD proteins, often larger than the protein of interest. Though not necessarily a major limitation in gap junction biology, the large size of GFP can interfere with the distribution, function, and fate of other recombinant proteins. GFPs offer no advantage over epitope tags for EM because both require conventional antibody labeling methods with the associated limitations in quality of preservation, reagent penetration, and labeling efficiency, all of which hinder specificity and resolution.

Recombinant proteins in intact cells can also be labeled by genetically appending or inserting a small motif (6 to 20 residues) containing the sequence -Cys-Cys-Xaa-Xaa-Cys-Cys-, then exposing the cells to a membrane-permeant nonfluorescent biarsenical derivative of fluorescein, FlAsH-EDT$_2$ (Fig. 1A). FlAsH binds with high affinity and specificity to the tetracysteine motif and thereby becomes strongly green fluorescent (12, 13). Toxicity and binding of the trivalent

[1]National Center for Microscopy and Imaging Research, Department of Neurosciences, 0608, [2]Department of Pharmacology, University of California, San Diego, 9500 Gilman Drive, La Jolla, CA 92093, USA. [3]Department of Anatomy and Cell Biology, University of Western Ontario, London, Ontario Canada, N6A 5C1

*Howard Hughes Medical Institute, University of California, San Diego, 9500 Gilman Drive, La Jolla, CA 92093–0648 USA.

†To whom correspondence should be addressed. E-mail: mhellisman@ucsd.edu

Fig. 1. Cx43-TC is expressed in HeLa cells and contributes to the formation of gap junction plaques. (**A**) Chemical structure of FlAsH-EDT$_2$ and ReAsH-EDT$_2$ ligands. (**B**) Schematic of the Cx43-TC construct. M1-4, transmembrane domains; E1-2, extracellular loop regions; CL, cytoplasmic loop; TC, tetracysteine domain; and a connexon hexamer with 6 ReAsH molecules bound to the tetracysteine domains. (**C**) Whole cell lysates from HeLa cells expressing Cx43-TC or wild-type Cx43 were Western blotted with a monoclonal antibody specific to Cx43. (**D** through **F**) pCI-neo-Cx43-TC was transfected in HeLa cells. Expression was checked 20 to 24 hours after transfection by double labeling with FlAsH-EDT$_2$ (D) and a Cx43-specific monoclonal antibody (E). Both labels recognized the same fusion protein, Cx43-TC as shown in (F). The cells were counterstained with propidium iodide (red) to highlight the cell bodies and nuclei. Bar, 5 μm.

arsenic atoms to endogenous thiols are minimized by simultaneous administration of micromolar concentrations of antidotes such as 1,2-ethanedithiol (EDT). More recently, we have determined in vitro rate constants for FlAsH association and dissociation from model tetracysteine-containing peptides to be in the range of 10^5 M^{-1}s^{-1} and 10^{-6}s^{-1}, respectively, consistent with effective dissociation constants around 10^{-11} M (14). Thus, once FlAsH-EDT$_2$ is present at micromolar concentrations in the cytosol, newly synthesized tetracysteine motifs should be labeled within a few minutes. Upon removal of excess FlAsH, the fluorescent complexes should survive for days in the absence of excessive (mM) concentrations of competing EDT. We have now synthesized red- and blue-emitting analogs, the most useful of which is ReAsH (Fig. 1A), a biarsenical derivative of the red fluorophore resorufin (14). Like FlAsH, ReAsH has very little fluorescence when bound to EDT, but becomes brightly fluorescent upon binding to tetracysteine motifs. Such complexes absorb and fluoresce at considerably longer wavelengths (593 and 608 nm, respectively) than the corresponding wavelengths (508 and 528 nm) for FlAsH complexes, even though ReAsH is a smaller molecule than FlAsH.

We engineered a recombinant connexin43 (Cx43), named Cx43-TC, by genetically fusing a 17 amino acid–long tetracysteine receptor domain (5′-EAAAREACCRECCARA-3′) (15) to the COOH terminus of Cx43 (Fig. 1B) (16). Cx43 is one of the best known and most widely distributed member of the connexin family, found in most mammalian organs. Fusions of GFPs to the COOH termini of connexins are functional, whereas analo-gous fusions to the NH$_2$ termini are nonfunctional (17). Cx43-TC was expressed in intercellular communication-deficient, Cx43-negative HeLa cells. Western blots of HeLa cells expressing Cx43-TC or wild-type Cx43 revealed that Cx43-TC migrated slightly slower than wild-type Cx43 reflecting the addition of the tetracysteine-tag (Fig. 1C). Fluorescent images of live cells stained with FlAsH-EDT$_2$ were virtually identical to the images of the same cells acquired after fixation, permeabilization, and staining with a Cx43-specific monoclonal antibody (Fig. 1, D through F) (18). Such congruence demonstrated that FlAsH staining was highly specific for the tetracysteine-tagged Cx43.

Cx43-TC assembles into functional gap junctions. Cx43-TC expressing HeLa cells were labeled with FlAsH-EDT$_2$ and then injected with Lucifer yellow (LY), which transferred within 1 to 5 s between contacting cells revealing that Cx43-TC had assembled into functional gap junctions. A large macromolecule, rhodamine dextran (molecular weight, 70 kD) did not pass through junctions and thus acted as a control to mark injected cells. Wild-type HeLa cells injected with LY did not show dye transfer at any time. A more quantitative measure of junctional competence was to record the electrical coupling by whole-cell patch clamping of each of the neighboring cells. Junctions consisting of Cx43-TC and labeled with FlAsH-EDT$_2$ had a mean conductance of 26 ± 16 nS (mean $\pm$ SD, $n = 18$), not significantly different ($P > 0.1$) from junctions formed from Cx43-GFP (32 ± 25 nS, $n = 8$) (19). Thus, the recombinant protein formed gap junctions, which were specifically recognized by FlAsH and whose ability to

transfer dye and electrical current was not affected by either the insertion of the tetracysteine receptor domain or by the labeling conditions and the binding of the ligand.

Gap junction dynamics. The ability to label Cx43-TC in live cells quickly and stoichiometrically with green FlAsH-EDT$_2$ and red ReAsH-EDT$_2$ enabled us to examine how Cx43 gap junction channels are added and removed from a gap junction plaque (20). We first labeled all preexisting Cx43-TC with FlAsH-EDT$_2$, then washed away unbound dye and incubated the cells for either a 4- (Fig. 2, A and B) or 8-hour (Fig. 2, C and D) interval. This labeling protocol pulse-labeled all preexisting Cx43-TC within the cell, but it would not label Cx43 molecules synthesized during the incubation interval of 4 or 8 hours. Subsequent labeling of the newly synthesized pool of Cx43-TC with red ReAsH-EDT$_2$ would not stain the older Cx43-TC molecules because their tetracysteine sites were still occupied by FlAsH. This pulse-chase labeling thus revealed the differential distributions of connexins synthesized at different times. The oldest proteins, stained green, were concentrated in the central region of the gap junction plaques flanked, as seen in thin optical sections, by two regions of red fluorescence from the most recently synthesized connexins. Three-dimensional reconstructions (Fig. 2, E through G) showed that the red regions were actually rings surrounding roughly circular green core zones. The partitioning between green and red fluorescence showed that younger protein molecules were added adjacent to older ones with remarkably little mixing. As the time interval between FlAsH-EDT$_2$ and ReAsH-EDT$_2$ applications was increased to 8 hours, the red periphery gradually displaced the central green core, leaving small intracellular punctae (presumably endocytic products) as the only remaining sites of green fluorescence (Fig. 2D). Other intracellular red punctae carrying young Cx43-TC might represent exocytic vesicles. As a control, the temporal order of FlAsH-EDT$_2$ and ReAsH-EDT$_2$ applications was reversed, which produced a reversed color pattern (Fig. 2H). Almost no intracellular punctae contained both colors, which is consistent with the separation of endocytic and exocytic traffic (Fig. 3A). Furthermore, young Cx43-TC were taken to the cell surface not necessarily in proximity to a preexisting plaque (Fig. 3A). Small junctions showed similar partition of green- and red-labeled Cx43-TC, indicating that the size of the plaque did not affect the segregation pattern of young and old protein (Fig. 3B). However, when two junctions were closely spaced, the segregation of green- and red-labeled Cx43-TC occurred asymmetrically so that the apposed portions of the plaques elongated less than the distal portions (Fig. 3C). This suggested that less

Fig. 2. FlAsH and ReAsH label two temporally separated pools of Cx43-TC and allow recording of junctional plaque renewal over time. HeLa cells stably expressing Cx43-TC were stained with FlAsH-EDT$_2$, incubated for 4 (**A** and **B**) or 8 (**C** and **D**) hours in complete medium at 37°C, stained with ReAsH-EDT$_2$, and imaged using a BioRad MRC-1024 confocal microscope. Panels (**A**) through (**D**) show Cx43-TC junctional plaques at different stages of refurbishing, as indicated by the different ratios of FlAsH (green) and ReAsH (red) stains. Panels (**E**) through (**G**) show a 3D volume projection of two Cx43-

TC containing plaques rotated through various angles, from 0° to 90° showing that the newer protein (red) is added as a ring around the periphery of existing junctions (green). Reversing the order of staining with FlAsH-EDT$_2$ and ReAsH-EDT$_2$ results in the reversal of the staining pattern (**H**), showing that the color pattern reflects the age of the connexin rather than any intrinsic bias of ReAsH-EDT$_2$ for connexins at the periphery or FlAsH-EDT$_2$ for connexins at the center of a plaque. Bars, 1 μm.
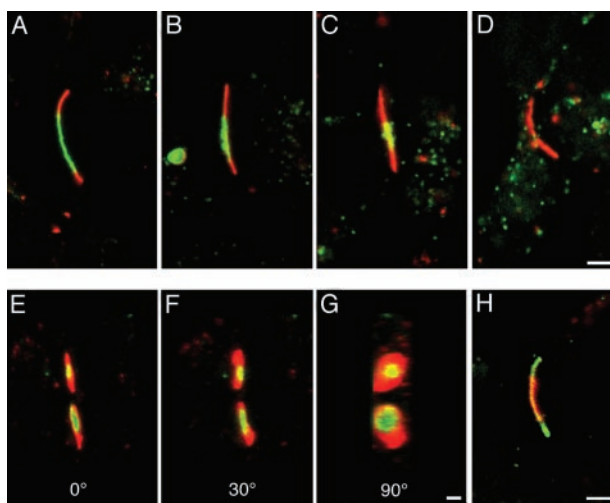
Cx43-TC is available in the smaller space between two adjacent plaques, reinforcing the hypothesis that new channels are transported to the plasma membrane and then flow to the sides of the plaque. Thus, under steady-state conditions of connexin expression, newly synthesized connexons are continually being taken to the cell surface, assembled into channels specifically at the edges of the gap junction; from there, they migrate in an orderly progression toward the center of the plaque, where they are removed by endocytosis. This inward radial flow is in the opposite direction from what is usually pictured at synapses, where central exocytosis is thought to be balanced by peripheral endocytosis (*21*).

Correlated electron microscopy. ReAsH is not only fluorescent but can also be used for photoconversion of diaminobenzidine (DAB) to allow direct correlation of live cell images with high-resolution EM detection (*22*). Photoconversion consists of intense illumination of a dye in fixed specimens in the presence of oxygen and DAB. Dye-catalyzed formation of singlet oxygen causes highly localized polymerization of DAB into an insoluble osmiophilic precipitate visible by EM (*23–25*). Previously, detection of specific macromolecules by photoconversion has required diffusion of antibodies, protein toxins, or antisense oligonucleotides into the fixed tissue (*25–28*). Neither GFPs nor FlAsH are capable of photooxidizing DAB with any efficiency. Live cells labeled with ReAsH could be imaged for long times at multiple focal planes with the use of confocal microscopy (Fig. 4A) or multiphoton excitation. Subsequent fixation with high concentrations of strong cross-linking fixatives such as glutaraldehyde (2%) did not affect the stability of the ReAsH-Cx43-TC complex (Fig. 4A). The fixed cells were then placed in a solution of oxygenated DAB, illuminated until a reaction product became visible by bright field microscopy, treated with osmium tetroxide, and prepared for EM. This preparation showed an electron-dense reaction product at the same gap junctions previously identified by fluorescence (Fig. 4B). At high magnification, structures corresponding in size and shape to individual channels at apposed plasma membranes were visible in cross sections of gap junction plaques (Fig. 4C). For comparison, a high-quality conventional immunogold image (Fig. 4D) showed that only a small, random fraction of the densely packed connexins were labeled. Maintenance of antigenicity and diffusional access of antibodies are antithetical to good ultrastructural preservation. By contrast, ReAsH-EDT$_2$ staining was performed while the cells were alive, enabling easy correlation of optical and EM images and the use of vigorous fixatives. The only molecules required for

the amplification process after fixation are oxygen, DAB, and osmium tetroxide, all of which are small and highly permeant.

Junctional trafficking. To begin characterizing how the traffic routes of nascent and senile connexins are spatially segregated at
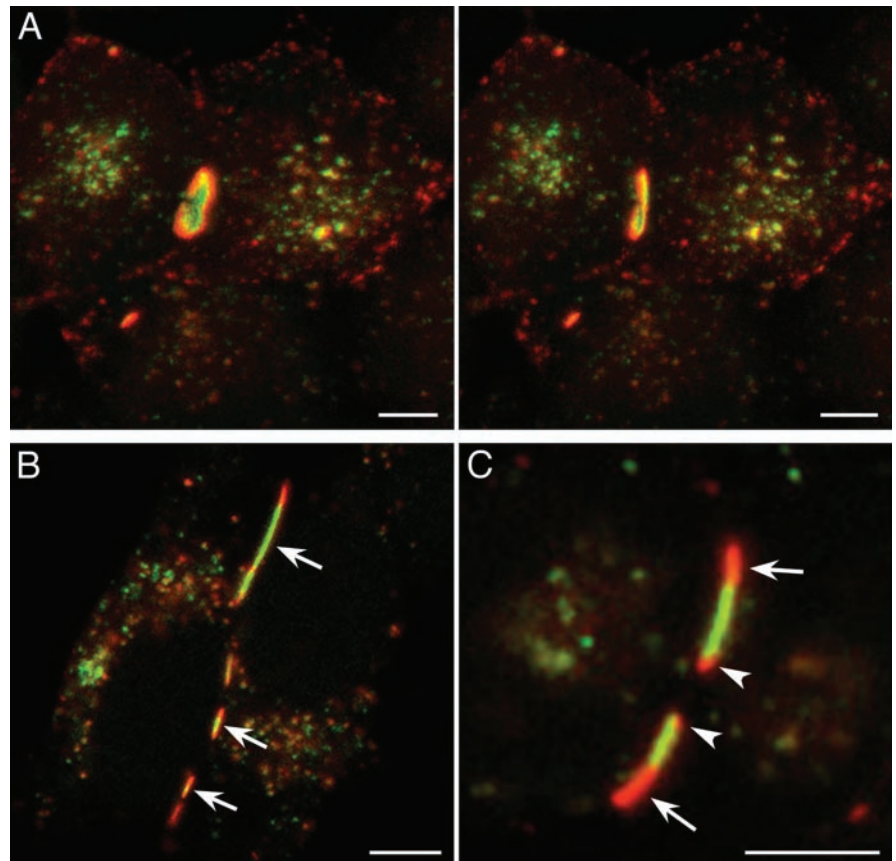
Fig. 3. Distribution, segregation and asymmetry of newer Cx43-TC in refurbishing plaques. Cells were labeled with FlAsH-EDT$_2$ (green) for 1 hour, incubated for 4 hours in complete medium at 37°C, stained with ReAsH-EDT$_2$, and imaged using a BioRad MRC-1024 confocal microscope. (**A**) Stereopair confocal image shows that the older protein is predominantly found in the center of a gap junction plaque and near the cell center (green), whereas the newer protein is found at the periphery of the plaque and dispersed in vesicles throughout the cytoplasm (red). These red vesicles can also be seen near the plasma membrane of both cells. (**B**) Plaques of different sizes (arrows) segregate similarly. (**C**) When two gap junctions occur in close apposition, an asymmetry in the segregation occurs with smaller areas of newly incorporated channels occurring at the proximal portions of the two plaques (arrowheads) and larger areas at the distal portions (arrows). Bars, 2 μm.

Fig. 4. ReAsH can photoconvert DAB to produce an electron dense reaction product allowing for tetracysteine-tagged connexins to be imaged in the same cells by both fluorescent and electron microscopy. (**A**) Confocal image of two ReAsH-labeled Cx43-TC containing gap junction plaques. (**B**) Electron micrograph of the same area after photoconversion. (**C**) The high magnification view of a portion of a

gap junction reveals dense packing of Cx43 hemichannels within gap junction plaques and highlights the high resolution obtainable with this labeling method. For comparison, a Lowicryl-embedded gap junction labeled for Cx43 with the traditional immunogold is shown in (**D**). Bar in (A) 10 μm, in (B) 1 μm, and in (C) and (D) 100 nm.
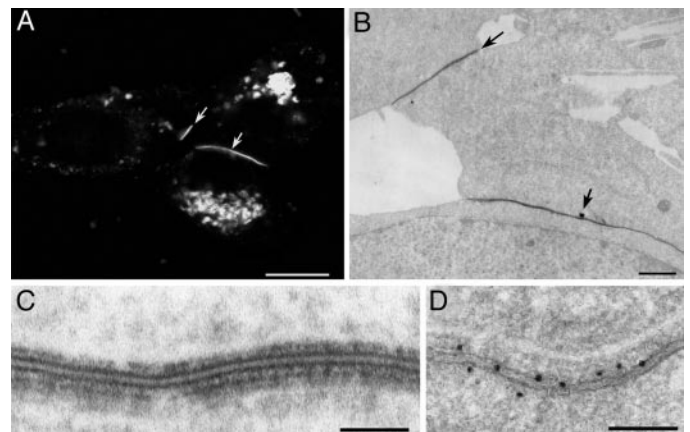
the ultrastructural level, it was desirable to image Cx43-TC within transport intermediates and organelles at EM resolution. The pulse-labeling protocol described earlier and the ability of ReAsH but not FlAsH to photooxidize DAB (as shown in Fig. 5, A through C) provided the opportunity to selectively examine older or newer connexons and their subcellular environment by EM. For example, if green FlAsH-EDT$_2$ incubation was followed 4 hours later by red ReAsH-EDT$_2$, then most recently synthesized red connexins could be followed preferentially throughout the exocytosis pathway by light microscopy and then be photoconverted and identified by EM. These presumably outbound vesicles typically ranged in size from 100 to 150 nm (120 ± 22.8, mean ± SD; $n =$ 53; area examined, 100 μm^2) and could be seen near the Golgi apparatus (Fig. 5D), dispersed throughout the cytoplasm (Fig. 5E) and fused to the plasma membrane (Fig. 5F). The distribution of these vesicles at various locations, not necessarily adjacent to an existing plaque, suggests that connexons go first to nonjunctional site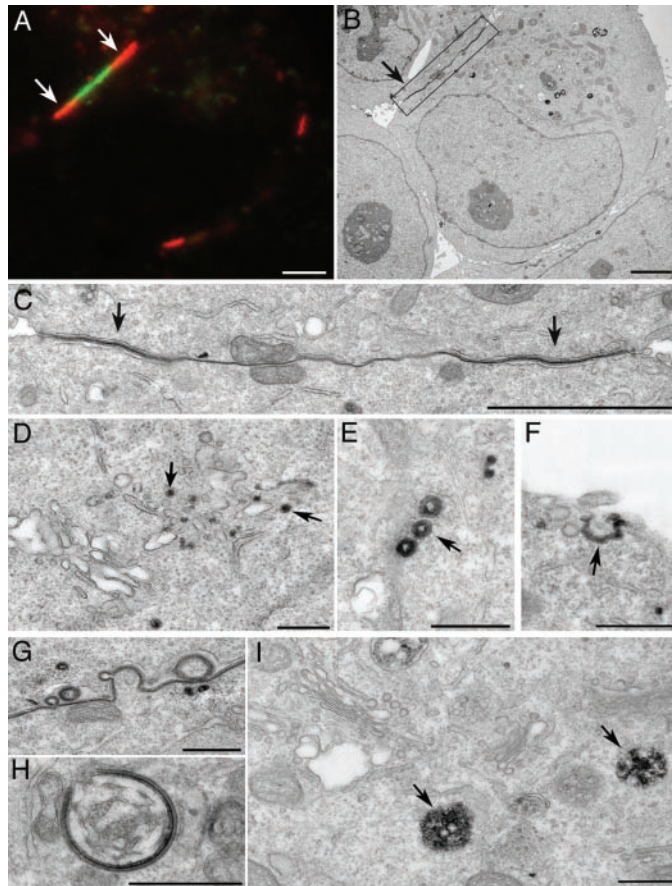s of the plasma membrane and then flow to the plaque. To highlight the Cx43 degradation pathway, Cx43-TC was labeled with ReAsH-EDT$_2$ and after 4 hours, newly synthesized Cx43-TC was labeled with FlAsH-EDT$_2$. The latter labeling step was not necessary for EM but was helpful for correlative fluorescence images. Internalization of plaque material could be visualized by EM (Fig. 5, G through I), which revealed stained lysosomal-like bodies (Fig. 5I). Some internalized gap junctions were clearly large double-membrane annular gap junctions, as previously described (Fig. 5H) (29), and internalized vesicles were quite variable in size.

Conclusions. The approach described here for studying the life cycle of proteins, including assembly and internalization, by correlated light and electron microscopy has considerable potential for generalization because the targeting motif is tiny, genetically encoded, and versatile. Previous techniques for distinguishing the age of a genetically encoded tag include the spontaneous green-to-red ripening of a mutated *Discosoma* fluorescent protein ("fluorescent timer") (30) and photobleaching or photoenhancement of *Aequorea* and *Discosoma* protein fluorescence (31–33). The spontaneous color change is elegantly simple but occurs gradually with a fixed time constant, so the time window of sensitivity is not easily manipulated, and abrupt boundaries such as in Fig. 2, A through C and E through G would be blurred. Moreover, aggregation of the DsRed prevents functional expression of many fusion proteins including connexin chimeras. The latter could only be rescued by cotransfection with an excess of unlabeled or GFP-labeled connexins (34). Optical marking of fluorescent proteins has faster time resolution but less contrast than our pulse-labeling protocol, whose ability to correlate multicolor with EM images is a unique advantage.

We have used this novel pulse-chase labeling approach at both the light and electron microscopy levels to show for the first time that gap junction plaques are assembled from the outer edges and removed from the central core. High-resolution images have revealed that 100- to 150-nm vesicles participate in the delivery of connexins to the cell surface. Gap junction internalization involves larger structures of more varied sizes and morphologies. These studies open avenues to uncover the complexity and sophistication of membrane protein assembly and turnover.

References and Notes

1. M. Yeager, B. J. Nicholson, *Curr. Opin. Struct. Biol.* **6**, 183 (1996).
2. G. Sosinsky, in *Gap Junctions, Molecular Basis of Cell Communication in Health and Disease*. C. Peracchia, Ed. (Academic Press, Rochester, NY, 2000), vol. 49, pp. 2–18.
3. D. A. Goodenough, J. A. Goliger, D. L. Paul, *Annu. Rev. Biochem.* **65**, 475 (1996).
4. L. S. Musil, A. C. Le, J. K. VanSlyke, L. M. Roberts, *J. Biol. Chem.* **275**, 25207 (2000).
5. D. W. Laird, *J. Bioenerg. Biomembr.* **28**, 311 (1996).
6. J. G. Beyer, E. C. Laing, in *Gap Junctions, Molecular Basis of Cell Communication in Health and Disease*, C. Peracchia, Ed. (Academic Press, Rochester, NY, 2000), vol. 49, pp. 24–42.
7. V. M. Berthoud, P. N. Tadros, E. C. Beyer, *Methods* **20**, 180 (2000).
8. P. E. Martin, J. Steggles, C. Wilson, S. Ahmad, W. H. Evans, *Biochem. J.* **350**, 943 (2000).
9. M. M. Falk, U. Lauf, *Microsc. Res. Tech.* **52**, 251 (2001).
10. M. M. Falk, *J. Cell Sci.* **113**, 4109 (2000).
11. K. Jordan *et al.*, *Mol. Biol. Cell* **10**, 2033 (1999).
12. B. A. Griffin, S. R. Adams, R. Y. Tsien, *Science* **281**, 269 (1998).
13. B. A. Griffin, S. R. Adams, J. Jones, R. Y. Tsien, *Methods Enzymol.* **327**, 565 (2000).
14. S. R. Adams *et al.*, *J. Am. Chem. Soc.*, in press. FlAsH and ReAsH are commercially available from PanVera Corporation, www.panvera.com.
15. Single-letter abbreviations for the amino acid residues are as follows: A, Ala; C, Cys; D, Asp; E, Glu; F, Phe; G, Gly; H, His; I, Ile; K, Lys; L, Leu; M, Met; N, Asn; P, Pro; Q, Gln; R, Arg; S, Ser; T, Thr; V, Val; W, Trp; and Y, Tyr.
16. Cx43 cDNA was subcloned in the prokaryotic vector Bluescript. The peptide Ala-Glu-Ala-Ala-Ala-Arg-Glu-Ala-Cys-Cys-Arg-Glu-Cys-Cys-Ala-Arg-Ala was fused to the COOH of Cx43 by polymerase chain reaction (PCR). The PCR product was sequenced to ensure fidelity and was subcloned into pCDNA3 (Invitrogen, Carlsbad, CA) at Not I (5′) and Xba I (3′) restriction sites. After amplification in DH5α′ *Escherichia coli* (Gibco-BRL, Invitrogen, Carlsbad, CA), the fusion gene

Fig. 5. Reaction products formed by the photoconversion of DAB by ReAsH allow detailed electron microscopy analysis of plaque refurbishing during double labeling experiments. When FlAsH-EDT$_2$ was used first to saturate preexisting Cx43-TC in transport vesicles as well as previously assembled gap junctions, ReAsH-EDT$_2$ only labeled newly synthesized recombinant Cx43. (**A**) Confocal image of a labeled junctional plaque. (**B**) Correlated EM image after photoconversion. (**C**) Higher magnification of the boxed region in (B), showing staining of the peripheral portions of the junction (arrows). (D) through (F) show staining of vesicles (arrows) associated with the Golgi apparatus (**D**), putative transport vesicles (**E**), and an exocytic event (**F**). By reversing the labeling order so that ReAsH was used first and was followed by an adequate incubation period in absence of free label, preexisting recombinant protein mainly associated to the degradative pathways and assembly intermediates were labeled, as shown in panel (**G** through **I**). Staining was observed at plaque material being internalized (G) and (H), and at lysosomal-like structures (I). Bars in (A) through (C) 2 μm and in (D) through (I) 0.5 μm.

was transfected into HeLa cells with Lipofectamine Plus (Gibco-BRL, Invitrogen). For transient expression experiments, cells were examined 20 to 24 hours after transfection. Stable expressing cells were obtained after approximately 2 weeks of selection in G418 (Gibco-BRL, Invitrogen) containing growth medium. Cx43-TC was also expressed in cardiac myocytes, NIH 3T3, and NRK cells, showing similar fluorescence patterns, trafficking, and functionality.

17. D. W. Laird et al., Microsc. Res. Tech. **52**, 263 (2001).
18. FlAsH-EDT$_2$ or ReAsH-EDT$_2$ was used at final concentrations of 1 and 2.5 μM, respectively, in presence of EDT (10 μM). The labeling was performed for one hour at 37°C in 1x Hank's Balanced Salt Solution (HBSS, Gibco-BRL, Invitrogen) supplemented with D$^+$ glucose (1g/l). Free and nonspecifically bound ligands were removed by washing with EDT (250 μM) (in HBSS+glucose). FlAsH-labeled cells were fixed with 4% formaldehyde (from paraformaldehyde), permeabilized, and stained with Cx43-specific monoclonal antibody (BD Biosciences, PharMingen, San Diego, CA).
19. Junctional conductance was measured with the use of the dual whole-cell patch clamp. Briefly, each cell of a pair is voltage clamped independently with a separate patch clamp amplifier (Axopatch-200A, Axopatch-200B. Axon Instruments, Union City, CA). By stepping the voltage in one cell and keeping the other constant, junctional current I_j is observed directly as a change in current in the unstepped cell. Thus, for stepping cell 1, g_j is obtained by dividing the change in I_2 by the change in V_1. Currents were digitized using Digidata 1200B (Axon Instruments) and analyzed with pCLAMP8 software (Axon Instruments). Pairs of gap junctions were randomly selected for recording. The large variance in conductance is due to a large variability in plaque size (proportional to varying numbers of active channels).
20. HeLa cells expressing Cx43-TC were labeled with FlAsH-EDT$_2$ or ReAsH-EDT$_2$ as described in (18). The unbound or nonspecifically bound ligand was removed by washing with astringent concentrations of EDT (250 μM, in HBSS) at the end of the labeling

time. Cells were then incubated for 4 to 8 hours in presence of complete medium. The newly synthesized recombinant proteins were stained in a second round of labeling, at the end of the 4 or 8 hour incubation time. The ligand used in the second round was either FlAsH-EDT$_2$ (for the cells initially labeled with ReAsH-EDT$_2$) or ReAsH-EDT$_2$ (for the cells initially labeled with FlAsH-EDT$_2$). The concentration of each ligand and the staining time were the same as in the first round of labeling. After washing, cells were either fixed in 4% formaldehyde (light microscopy imaging) or 2% glutaraldehyde (electron microscopy imaging) or were imaged live (using either a BioRad MRC-1024 confocal microscope or a BioRad RTS2000 video rate laser-scanning microscope operating in two-photon mode) in HBSS supplemented with glucose and EDT (10 μM). The use of a BioRad RTS2000 was particularly useful for recording of time-lapse movies. Because the RTS2000 can acquire optical sections at high frame rates, it is possible to record 3D volumes quickly and follow the labeled proteins in 3D over long periods of time (4D). This multiphoton system was used to record 4D data from the Cx43-TC expressing HeLa cells for up to 6 hours.
21. J. E. Heuser, T. S. Reese, J. Cell Biol. **57**, 315 (1973).
22. Photoconversion of DAB. After labeling with ReAsH-EDT$_2$ and live cell imaging, the cells were fixed with 2% glutaraldehyde in sodium cacodylate buffer (0.1 M) (pH 7.4) for 20 min, rinsed in buffer and treated for 5 min in KCN (20 mM), aminotriazole (5 mM), glycine in buffer (50 mM) to reduce nonspecific background. For photoconversion, diaminobenzidine (1 mg/ml) in oxygenated sodium cacodylate (0.1 M) was added to the culture dish and the cells were irradiated with 585-nm light from a xenon lamp for 10 to 15 min until a brownish reaction product appeared in place of the red fluorescence. Cells were then washed in buffer and post-fixed in 1% osmium tetroxide for 30 min. Cells were rinsed in distilled water, dehydrated in ethanol, embedded in Durcupan resin, and polymerized at 60°C for 48 hours.
23. P. A. Takizawa et al., Cell **73**, 1079 (1993).
24. A. R. Maranto, Science **217**, 953 (1982).

25. T. J. Deerinck et al., J. Cell Biol. **126**, 901 (1994).
26. F. Capani et al., J. Histochem. Cytochem. **49**, 1351 (2001).
27. S. Huang, T. J. Deerinck, M. H. Ellisman, D. L. Spector, J. Cell Biol. **126**, 877 (1994).
28. M. E. Martone, T. J. Deerinck, N. Yamada, E. Bushong, M. H. Ellisman, J. Histotechnol. **23**, 261 (2000).
29. K. Jordan, R. Chodock, A. R. Hand, D. W. Laird, J. Cell Sci. **114**, 763 (2001).
30. A. Terskikh et al., Science **290**, 1585 (2000).
31. J. Lippincott-Schwartz, E. Snapp, A. Kenworthy, Nature Rev. Mol. Cell. Biol. **2**, 444 (2001).
32. J. S. Marchant, G. E. Stutzmann, M. A. Leissring, F. M. LaFerla, I. Parker, Nature Biotechnol. **19**, 645 (2001).
33. H. Yokoe, T. Meyer, Nature Biotechnol. **14**, 1252 (1996).
34. U. Lauf, P. Lopez, M. M. Falk, FEBS Lett. **498**, 11 (2001).
35. We wish to thank M. E. Martone for helpful suggestions, discussions, and critical reviewing of the manuscript; K. Jordan for providing pBluescript-Cx43; A. Han for skillful help with the construction of Cx43-TC and its expression in HeLa, NRK cells, and in cardiac myocytes; M. Shah for helpful discussion and for the dye injection experiments and expression in cardiac myocytes; M. M. Falk for helpful discussions and for providing the Cx43-GFP construct used in the electrical coupling experiments; A. Hand for assistance with the immunogold EM. The work described here was conducted at the National Center for Microscopy and Imaging Research at San Diego, which is supported by National Institutes of Health Grant RR04050 awarded to M.H.E. This work is also supported by the Howard Hughes Medical Institute, DOE contract DE-DE-AC03-76SF00098, and NIH grant NS27177 to R.Y.T., NIH grants NS14718 and DC03192 to M.H.E., National Science Foundation MCB-9728338 (to G.E.S.), the Canadian Institutes of Health Research (MT-12241, awarded to D.W.L.). S.R.A. was supported in part by the National Institute of Health grant PO1 DK54441 (awarded to S. S. Taylor).

REPORTS

Ordering in a Fluid Inert Gas Confined by Flat Surfaces

Stephen E. Donnelly,[1]* Robert C. Birtcher,[2] Charles W. Allen,[2] Ian Morrison,[1] Kazuo Furuya,[3] Minghui Song,[3] Kazutaka Mitsuishi,[3] Ulrich Dahmen[4]

High-resolution transmission electron microscopy images of room-temperature fluid xenon in small faceted cavities in aluminum reveal the presence of three well-defined layers within the fluid at each facet. Such interfacial layering of simple liquids has been theoretically predicted, but observational evidence has been ambiguous. Molecular dynamics simulations indicate that the density variation induced by the layering will cause xenon, confined to an approximately cubic cavity of volume $\approx$ 8 cubic nanometers, to condense into the body-centered cubic phase, differing from the face-centered cubic phase of both bulk solid xenon and solid xenon confined in somewhat larger ($\geq$20 cubic nanometer) tetradecahedral cavities in face-centered cubic metals. Layering at the liquid-solid interface plays an important role in determining physical properties as diverse as the rheological behavior of two-dimensionally confined liquids and the dynamics of crystal growth.

Theoretical investigations of the structure of liquids at solid interfaces have indicated that density modulation perpendicular to the interface is likely to occur (1–5). Such layering is expected to occur even in simple hard-sphere systems and results from the geometrical constraining effect of the solid surface on the atoms or molecules of the liquid, which causes them to order into quasi-discrete layers (6). Recent x-ray scattering experiments on supercooled liquid Ga (7) and an organic liquid (8) have revealed the presence of a small number of distinct layers; however, in the former case dimerization may play a role and in the latter the liquid consists of complex polyatomic molecules, complicating interpretation. We report high-resolution transmission electron microscopy (HRTEM) observations of the interface structure in room-temperature, fluid Xe (critical temperature 16°C) confined in small faceted cavities in electron-transparent Al. Molecular dynamics (MD) simulations provide further insights into the behavior of this simple fluid in small cavities.

HRTEM is a powerful technique for probing the structure of interfaces such as grain boundaries and free surfaces in solids but is generally not suitable for studying the structure of interfaces involving liquids. In addi-

[1]Joule Physics Laboratory, Institute for Materials Research, University of Salford, Manchester M5 4WT, UK. [2]Materials Science Division, Argonne National Laboratory, Argonne IL 60439, USA. [3]National Institute for Materials Science, 3-13 Sakura, Tsukuba 305, Japan. [4]National Center for Electron Microscopy, LBNL, Berkeley, CA 94720, USA.

*To whom correspondence should be addressed. E-mail: s.e.donnelly@salford.ac.uk